A PRELIMINARY EXPERIMENTAL INVESTIGATION OF THE FLOW OVER SIMPLE BODIES OF REVOLUTION AT M = 18.4 IN HELIUM

Thesis by

Albert G. Munson

In Partial Fulfillment of the Requirements

For the Degree of

Aeronautical Engineer

California Institute of Technology

Pasadena, California

1956

ACKNOWLEDGMENTS

The author wishes to express his sincere appreciation to his advisor, Professor Lester Lees, for his help and encouragement throughout this work. He is also greatly indebted to Dr. H. T. Nagamatsu for his interest and suggestions, especially during the early part of the work.

The help of the hypersonic staff in carrying out the tests is greatly appreciated.

Thanks are also due to Mr. W. M. Sublette for his most skillful work in making the models.

Appreciation is also expressed to Mrs. H. Van Gieson for typing the thesis and to Mrs. C. Kelley and Mrs. M. Wood for preparing the figures.

ABSTRACT

An experimental investigation was conducted in the GALCIT hypersonic blow-down tunnel to determine surface pressure distributions and shock wave shapes for a series of "sharp" nosed and slightly blunted bodies of revolution at nominal Mach number of 18.5 and a free stream Reynolds number of 4.75×10^5 per inch. The four bodies investigated were as follows: (1) 15° half-angle "sharp" cone; (2) 15° half-angle spherically-blunt cone (bluntness ratio = .24); (3) 20° half-angle "sharp" cone; and (4) 2/3 power body.

The pressure distributions on the "sharp" cones agreed well with the Taylor Maccoll theory. The pressure near the nose of the blunt cone was much higher than that predicted by the theory, as is expected, but decreases monotonically to a value lower than the theoretical value, indicating that the flow has over expanded. The measured shock wave shape for the 2/3 power body was found to be proportional to $x^{0.69}$, and the shock wave ordinates agree very closely with those predicted by Cole.

TABLE OF CONTENTS

LIST OF FIGURES

LIST OF SYMBOLS

C_p	pressure coefficient $\dfrac{p - p_\infty}{\frac{1}{2} \rho_\infty U_\infty^2}$
L	body length
M	Mach number
p	pressure
p_o	total pressure
p_o'	total pressure behind a normal shock
r	radial distance
r_{max}	maximum body radius
r_n	nose radius of spherically-blunt cone
s	distance from nose measured along body surface
u	speed
x	distance from nose measured along body axis
γ	ratio of specific heats at constant pressure and volume, C_p/C_v
θ	flow deflection angle
θ_c	cone half angle
ρ	density
∞	refers to free stream conditions

I. INTRODUCTION

At hypersonic flight speeds the gas temperatures near the surface of a body are sufficiently high so that chemical (and possibly electronic) phenomena play an important part in determining the flow field. Because of the complexity of the complete problem, it seems worthwhile to study hypersonic flows in much simpler gases than air, in order to bring out the purely fluid-mechanical effects associated with strong, highly curved shocks and thick boundary layers. For this purpose helium offers an attractive solution as a wind tunnel working fluid. Helium obeys the perfect gas law and its specific heat is practically constant over a wide range of temperatures and pressures. In addition, the transport properties of helium are well established. The liquefaction temperature of helium is about $1.5^{\circ}K$ at a pressure of 0.004 atmospheres, for example, so that Mach numbers of the order of 20 can be produced without the necessity of pre-heating the gas to avoid condensation.*

So far as is known, F. K. Hill (Ref. 1) at the Applied Physics Laboratory was the first to utilize helium as a wind tunnel working fluid. More recently, Hammitt (Ref. 2) and Bogdonoff at Princeton studied the flow around some simple bodies in helium in the range $11 < M < 13$, with particular emphasis on leading-edge effects. Their results show that the influence of a blunt leading-edge on a flat plate

---

* There are also secondary advantages, such as the fact that the isentropic area ratio at a given Mach number and the total head loss across a normal shock are both much lower in helium than in air.

extends many hundreds of leading-edge thicknesses downstream at hypersonic speeds. Lees (Ref. 3) shows theoretically that in this case the inviscid transverse flow field exhibits certain similarity properties typical of a "constant-energy" flow behind an expanding, strong shock wave. The shape of the bow shock wave R(x) not too close to the nose is given by $R/d = K_1(\gamma)(x/d)^{\frac{1}{2}}$ for a body of revolution, and by $R/d = K_o(\gamma)(x/d)^{2/3}$ for a cylindrical body. This last result agrees closely with the experimental results of Hammitt and Bogdonoff. Flow similarity is also possible for a class of bodies of the form $r_b \sim x^m$, provided that $m' \leq m \leq 1$, where $m' = 3/4$ for cylindrical body and $m' = 3/2 \frac{\gamma + 1}{3\gamma + 2} \simeq 0.60$ for a body of revolution. In his study of Newtonian flow around slender bodies of arbitrary shape, J. D. Cole (Ref. 4) also considered the family $r_b \sim x^m$ as a special case. Here the parameter $\gamma - 1/\gamma + 1$ is small, and the Newtonian parameter $(\gamma - 1) M_\infty^2 \theta^2$ must be of the order 1 - 2 or larger. In order for the surface pressure to be non-negative $m \geq \frac{1}{2}$ for a cylindrical body and $m \geq 1/3$ for a body of revolution.

The present investigation in the GALCIT helium tunnel was undertaken to provide experimental data on shock wave shapes and surface pressure distributions for some simple "sharp"-nosed and slightly-blunted bodies of revolution at a nominal Mach number of 18.5. The bodies selected were two sharp-nosed cones of 15^o and 20^o half-angle, a 15^o half-angle cone with a nose bluntness ratio of 0.24, and a body of the form $r/r_{max} = (x/L)^{2/3}$, which is the hypersonic optimum shape, or body of minimum wave drag for a given fineness ratio, including the effect of centrifugal force. This investigation was sponsored by the U. S. Army Ordnance and the Office of Ordnance Research, under Contract No. DA-04-495-Ord-19.

II. EQUIPMENT AND PROCEDURE

A. Equipment

1. Wind Tunnel Description

Two hypersonic helium tunnels have been described in detail in the literature (Refs. 1 and 2). Both are axially-symmetric blow-down tunnels with conical nozzles. The helium tunnel constructed at Johns Hopkins University has a nozzle cone angle of 10^{o} and a test section diameter of approximately 1.94 inches. The source of working fluid is high pressure bottled gas. When nitrogen is used the test section Mach number is approximately 9.1. This tunnel has been used for studies of the supersaturation of nitrogen in hypersonic wind tunnels and for studies of boundary layers in hypersonic flow.

The helium tunnel at Princeton University has a nozzle angle of 11^{o} and a test section diameter of 3-1/4 inches. The helium is obtained in tank semi-trailers which are used as a high pressure storage system. An air operated ejector is used to evacuate the diffuser. The test section Mach number range is 11 to 15 and the Reynolds number ranges from 0.6×10^{6} to 1.8×10^{6} per inch, approximately. This tunnel has been used for shock wave boundary layer interaction problems on such bodies as flat plates, cones, and wedges.

The present investigation was conducted in the GALCIT hypersonic blow down tunnel utilizing bottled helium as a high pressure source of working fluid. The diffuser was connected to the GALCIT hypersonic wind tunnel plant. This plant consists of thirteen rotary vane-type positive displacement compressors and three reciprocating

piston type compressors. For the present investigation the plant was operated with five stages of compression using the thirteen vane-type compressors only. The helium was not heated so that the stagnation temperature was about 520°R. The range of stagnation pressures was 500 psi to 1500 psi, the Mach number ranged from 17 to 19.4, and the Reynolds numbers varied from 2.50×10^5/inch to 7.0×10^5/inch in the test section. The operating compression ratio of the wind tunnel (i.e., p_o/p_o') was 1500 to 2000, or five to seven times the equivalent ratio across a normal shock at $M_\infty = 19$. With 3 bottles available, the running time of the wind tunnel was one to two minutes.

A sketch of the helium tunnel is shown in Figure 1. The nozzle is an axially-symmetric brass cone with a throat diameter of .050 inches, an exit diameter of 1.676", and a total cone angle of 10°. The center section, also made of brass, is approximately 7 inches long and butts directly to the nozzle. This section has parallel walls with a diameter of 1.676 inches for the first 8.9 inches of its length, and tapers linearly to a 2.0 inch diameter. Windows 3 inches long and 1 inch high are mounted 2.0 inches from the beginning of the straight section. The diffuser section, which is 2.0 inches in diameter, bolts directly to the downstream end of this center section. The diffuser section has been offset to facilitate the design of a hand-actuated axial traverse system.

2. Wind Tunnel Operation and Control

With no helium flow, the nozzle, diffuser, and piping were evacuated to a pressure of two to three mm. Hg abs. To establish

supersonic flow with most models it was found necessary to start the tunnel with the model located about one inch downstream of the throat, and then withdraw the model slowly to the desired location in the test section.

The stagnation pressure was measured with an Ashcroft Laboratory test gage which has a capacity of 1500 psi and is subdivided into 10 psi increments. The stagnation pressure was controlled by a high pressure gas regulator manufactured by the Victor Equipment Company of San Francisco, California. This regulator allowed a variation of $\pm$ 5 psi at most in 2 minutes running time. Since all tests were made at either 1000 psi or 800 psi this variation amounts to about $\pm \frac{1}{2}$ per cent in p_o.

3. Description of Instrumentation

a. Manometer

Pressures were measured by a fourteen-tube silicone manometer referenced to a very low pressure (Ref. 5). The reference pressure was measured with an ionization gage called the "Alphatron", which indicated that this pressure was approximately 20 microns or .020 millimeters of mercury. This value is about 2 per cent of the static pressure measured on the nozzle side wall, and 0.05 per cent of the lowest static pressure measured on the models.

b. Wind Tunnel Pressure Instrumentation

Pitot pressures were measured with a single tube .083 inches in diameter, and also with a two-tube rake in which each tube has a

diameter of .040 inches. Within the accuracy of the pressure measurements these two instruments gave the same result. Both were supported from the rear in the same manner as models were supported. (See II. B. 1.) Five static pressure orifices .013 inches in diameter were placed in the nozzle in the locations given below. (Here x is the distance from the throat and L is the nozzle length.)

Orifice	x/L
1	.149
2	.443
3	.577
4	.705
5	.839

c. Schlieren Apparatus

A sketch of the schlieren system is shown in Figure 2. The light source is an AH-4 mercury vapor lamp and the parabolic mirror has a focal length of 4 ft. Since the negative lens is placed between the knife edge and the camera, its only function is to increase the size of the image. Schlieren photographs were taken with a camera shutter speed of 1/50 second.

Because of the fact that helium gas has a very low index of refraction the schlieren system used here was barely adequate to photograph the shock wave configuration around the model. It was found possible with proper combinations of exposing, developing, and printing to photograph segments of shock waves which were too faint to be viewed on a ground glass screen. In general it was found desirable to underexpose slightly in order to obtain a negative which was not very

dense. Negatives of this type seemed to have considerably more contrast than negatives of normal density. High contrast developer was used and printing was done on high contrast paper.

4. Wind Tunnel Flow Calibration

Total pressure distributions across the nozzle were measured at three axial stations; station 1 lies 1.44 inches upstream of the nozzle exit, station 2 is located at the nozzle exit, and station 3 is located in the center section 2.14 inches downstream of the nozzle exit. These results (Fig. 4) show that the thick wall boundary layer reduced the effective working area of the wind tunnel by a factor of 4. The total pressure and Mach number vary $\pm$ 8 per cent and $\pm$ 2.8 per cent respectively across the working section. The axial variation in Mach number is about 0.7 per inch.

It is evident that if the model tested is small enough the variation in Mach number and total pressure across the space it occupies is small. The total pressure variation across a model with 0.313 inch base diameter is $\pm$ 1$\frac{1}{2}$ per cent. If the model is 0.5 inches long the axial Mach number variation is 0.35. This flow is considered sufficiently uniform for a preliminary investigation.

5. Model Description

A description of the models tested and their principal dimensions is given in the following table; (All models were made of brass.)

Model	Base Diameter (Inches)	Length (Inches)	Nose Diameter (Inches)
15^{o} Half-Angle "Sharp" Cone	.313	0.582	.010
15^{o} Half-Angle Spherically-Blunt Cone	.313	0.480	.075
20^{o} Half-Angle "Sharp" Cone	.281	0.385	.001
2/3 Power Body $(r/r_{max}) = (x/L)^{2/3}$	.313	0.50	.004

Each model was fitted to a cylindrical afterbody of the same base diameter as the base diameter of the model and approximately three inches long. The models were supported by a sting of 1/4 inch diameter from the rear which contained all the pressure leads. Each model except the 2/3 power body contained five pressure orifices spaced as follows: (s is the distance from the nose measured along the body surface.)

a. 15^{o} Half-Angle "Sharp" Cone (See Fig. 3.)

Orifice	s''
1	0.030
2	0.150
3	0.270
4	0.380
5	0.510

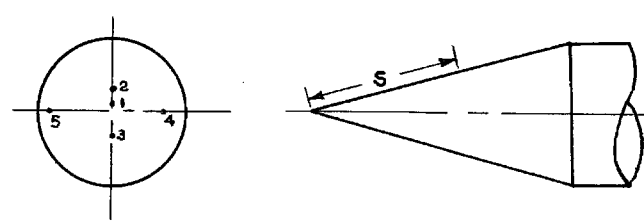

b. 15° Half-Angle Spherically-Blunt Cone

Orifice	s''
1	0.050
2	0.085
3	0.140
4	0.210
5	0.360

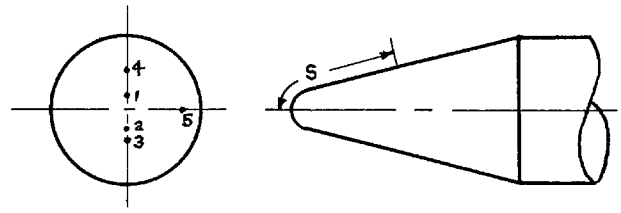

c. 20° Half-Angle "Sharp" Cone

Orifice	s''
1	0.050
2	0.130
3	0.210
4	0.290
5	0.370

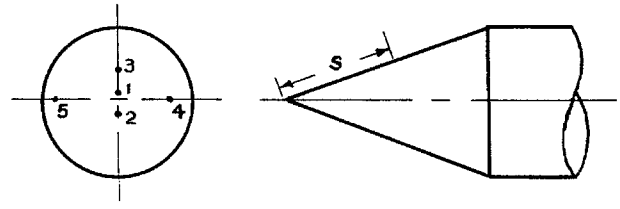

B. Procedure

1. Model Mounting and Leak Check

All models were supported by stings approximately 40'' long, and the stings in turn were mounted at two points: The first support point was $9\frac{1}{2}$ inches from the nozzle exit, and this support can be

moved both horizontally and vertically. The other support, which was located at the point where the sting passed through the side of the z-shaped diffuser section (See Figure 1.), consisted of a small metal plate with a 1/4" hole drilled through it and an 0-ring groove cut inside the hole. Thus this plate acted both as a support and as a seal. The plate was bolted to a machined flat section on the z-shaped diffuser. A 1/8" hole was drilled through this flat section so that the sting could pass through both holes. This mounting gave a small amount of adjustment to the rear support, and the models could be placed at any distance from the axis of symmetry of the tunnel with any desired angle of attack. The end of the sting was gripped by a brass guide which was free to slide between two stops. These stops set the limits of axial movement of the model in the wind tunnel.

The pressure leads were brought outside the wind tunnel through the sting and connected directly to saran tubing which led to the manometer. Leak checking was performed by evacuating the pressure lead and manometer tube, then clamping off the vacuum pump. A pressure rise in the system, indicating leakage, was shown by a movement of the manometer fluid. A movement of one centimeter of silicone in two hours was considered sufficiently small for the present preliminary investigation.

For static pressure measurements the models were located at the end of the nozzle section. For schlieren observations the models had to be located farther downstream between the windows in the center section. A new center section, identical to the first except that the

windows are located 1-1/4 inches farther upstream, was constructed. This was done so that the model could be placed near the end of the nozzle where the flow was reasonably uniform. The models were then located .9 inches downstream of the end of the nozzle.

2. Static Pressure Measurement

Model static pressures were measured with the silicone oil manometer described earlier. The response time of this manometer was measured in the following manner: Each model was placed in a vacuum chamber and its pressure leads connected to the manometer. Each manometer tube was equipped with a valve which sealed off the tube. The vacuum chamber was then evacuated to the expected model pressure, and the valves were opened and the time for each tube to reach equilibrium was recorded. With this arrangement the manometer tubes can be set at any desired pressure level initially. When the initial pressure set in the manometer tube was within 15 per cent of the pressure in the vacuum chamber, it was observed that less than one minute was required for the pressure in the tube to approach within 1 per cent of the pressure in the vacuum chamber, i.e., the "time lag error" of the manometer is less than 1 per cent. All wind tunnel tests were run for more than one minute.

The first model (15° half angle "sharp" cone) was tested in three angular positions spaced 90° apart around the model axis. In all cases the model was located on the centerline of the wind tunnel and the model axis lined up with the tunnel axis. From the nature of the initial data obtained, however, it was evident that scatter was

caused by flow inclination in the wind tunnel. For hypersonic flow over slender bodies

$$C_p \sim \theta^2$$

where C_p is the pressure coefficient $\dfrac{p - p_\infty}{\frac{1}{2} \rho u_\infty^2}$, and θ is the angle of flow deflection. Therefore,

$$\frac{\Delta p}{p} = \frac{2 \Delta \theta}{\theta}$$

Here $\Delta p/p$ was obtained from the experimental data and $\Delta \theta$ was calculated from the above formula. The result found is that the flow is inclined downward in the vertical plane at an angle of 0.4°. There is no flow inclination in the horizontal plane. The model was then pitched upward 0.4°.* The tests were repeated and a considerable decrease in scatter of the data resulted. All subsequent tests were run at 0.4° pitch.

---

* Since the two model supports described earlier did not have sufficient travel to permit the model to be pitched by this amount, and at the same time be placed on the wind tunnel centerline, the sting supports were bent slightly.

III. DISCUSSION OF RESULTS

A. Static Pressure Measurements

1. Sharp-Nosed 15° and 20° Half-Angle Cones

Lees (Ref. 6) has obtained an approximate relation giving pressure distribution on an unyawed cone in hypersonic flow. The approximation can be considered valid for $M_\infty > 4$ and $(1/M_\infty) < \theta_c < \overline{\theta}$ where $\overline{\theta} \cong 28^\circ$ corresponds to the upper limit of the "zone" of hypersonic similarity. The present experiments fall within this range. The pressure distribution for the 15° half-angle sharp cone is given in Figure 9, and the agreement with the theory is in general considered good. The difference between the calculated pressure coefficient and that observed for the first orifice may be caused by the fact that it is located only three nose diameters downstream of the slightly blunt (0.010" diameter nose). The inconsistency in the two pressures measured by the third orifice is not understood. The difference in pressures is far larger than the experimental errors. One possible explanation is that a wave is present in the wind tunnel which strikes the model only on one side.

The results for the 20° half-angle sharp cone are presented in Figure 10. The experimental values agree closely with cone theory. The scatter in the experimental points is about twice the estimated experimental error.

At the Mach numbers and Reynolds numbers in the flow behind the shock there is no evidence of boundary layer-shock wave interaction.

2. 15° Half-Angle Spherically-Blunt Cone

As shown in Figure 11, the pressures near the nose are high, as

expected, but decrease monotonically to values below the predicted asymptotic pressures for a semi-infinite cone. The pressure measured at the point of tangency of the spherical nose and the cone is more than twice the pressure measured on the 15^{o} sharp cone. The pressures at a distance of six nose radii downstream on the cone are approximately twenty five per cent lower than the pressure measured on the sharp cone. Over-expansions on bodies as slender as this one are not observed in experiments in air ($\gamma = 1.4$) at Mach numbers of the order of 6 (Ref. 7). These differences between the behavior in helium and in air have not yet been explained.

B. Schlieren Observations

1. 15^{o} Half-Angle Spherically-Blunt Cone

Figure 6 is a schlieren photograph of the 15^{o} half-angle spherically-blunt cone at a free stream Mach number of 18.4. The detached bow wave is very close to the nose of the body. Within the field of view (axial distance 18 nose radii downstream) the bow shock wave is curved and the shock wave angle has not yet reached the asymptotic value corresponding to the semi-infinite 15^{o} cone.

2. 2/3 Power Body

Figure 7 is a schlieren photograph of the 2/3 power body at the same free stream conditions as those for the spherically-blunt cone described above. The bow shock wave lies very close to the body surface, and the radial distance of the shock from the body axis as measured by means of an optical comparator was found to be proportional to $x^{0.69}$ (Fig. 8). This result is in good agreement with the theoretical predictions of Cole. (See Section I.)

REFERENCES

1. Hill, F. K.: Boundary Layer Measurements in Hypersonic Flow. Journal of the Aeronautical Sciences, Vol. 23, No. 1, pp. 35-42, January, 1956.

2. Bogdonoff, S. M., and Hammitt, A. G.: Fluid Dynamic Effects at Speeds From M = 11 to 15. Journal of the Aeronautical Sciences, Vol. 23, No. 2, pp. 108-116, February, 1956.

3. Lees, L.: Inviscid Hypersonic Flow over Blunt-Nosed Slender Bodies. California Institute of Technology, Guggenheim Aeronautical Laboratory, Memorandum No. 31, February 1, 1956.

4. Cole, J. D.: Newtonian Flow Theory for Slender Bodies. RAND Corporation, Report No. RM-1633, February 13, 1956.

5. Nagamatsu, H., and Willmarth, W.: Condensation of Nitrogen in a Hypersonic Nozzle. California Institute of Technology, Guggenheim Aeronautical Laboratory, Memorandum No. 6, January 15, 1952.

6. Lees, L.: Note on the Hypersonic Similarity Law for an Unyawed Cone. Journal of the Aeronautical Sciences, Vol. 18, No. 10, pp. 700-702, October, 1951.

7. Machell, R. M., and O'Bryant, W. T.: An Experimental Investigation of Hypersonic Flow over Blunt Nosed Cones at a Mach Number of 5.8. California Institute of Technology, Guggenheim Aeronautical Laboratory, Memorandum No. 32, 1956.

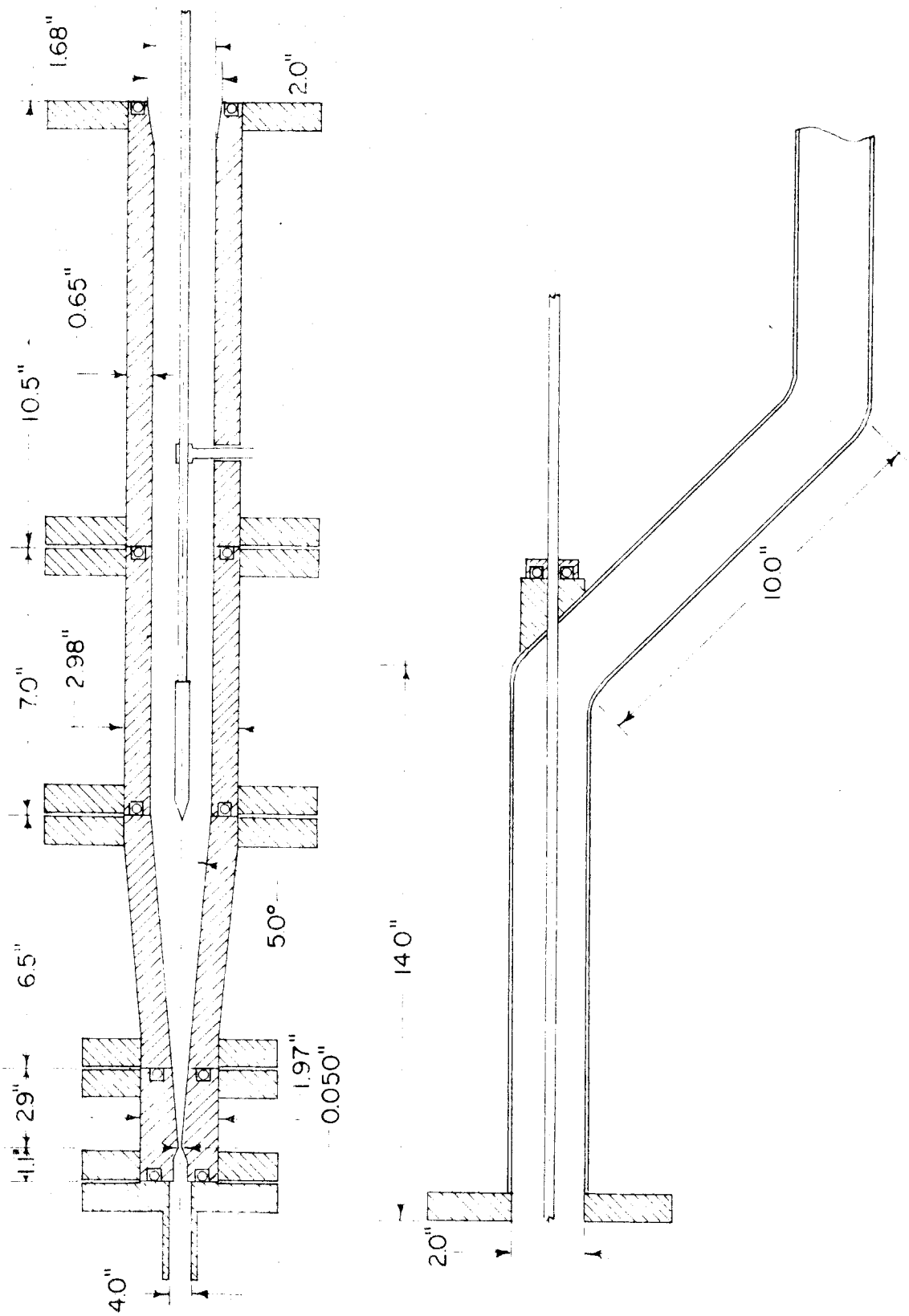

FIG. 1 CROSS SECTION OF AXIAL SYMMETRIC NOZZLE AND DIFFUSER

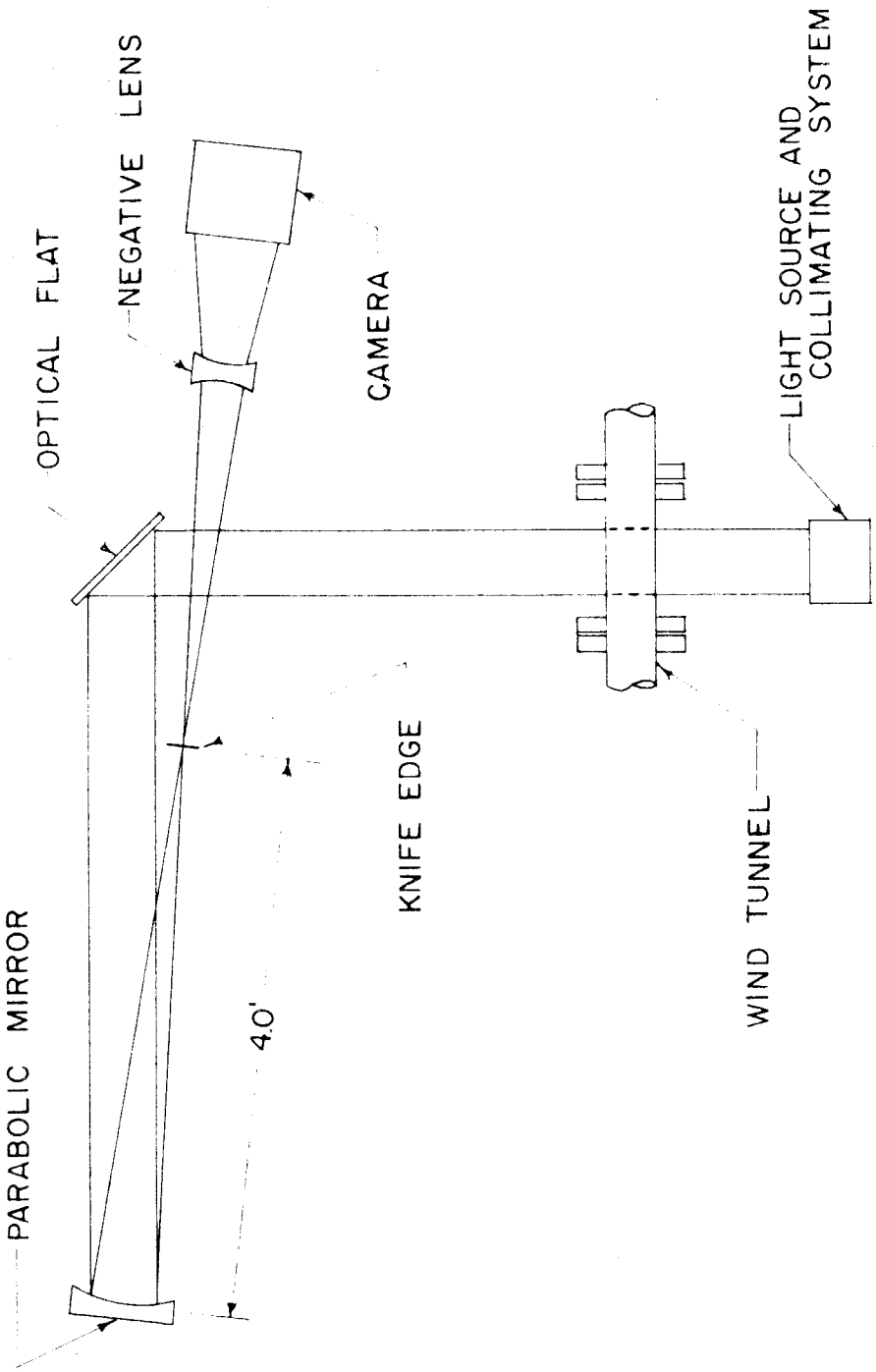

FIG. 2 SCHEMATIC OF SCHLIEREN SYSTEM

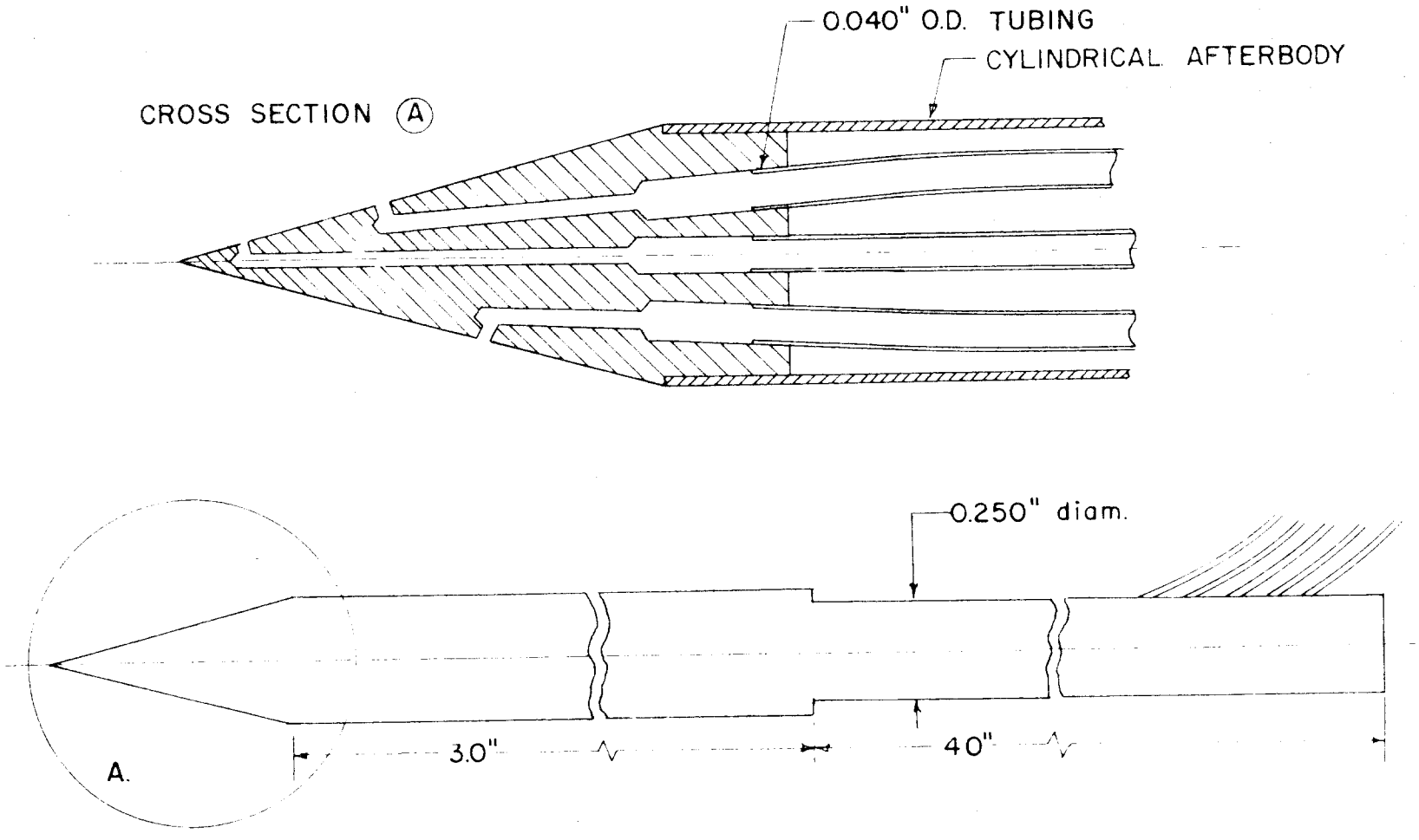

FIG. 3 TYPICAL PRESSURE MODEL

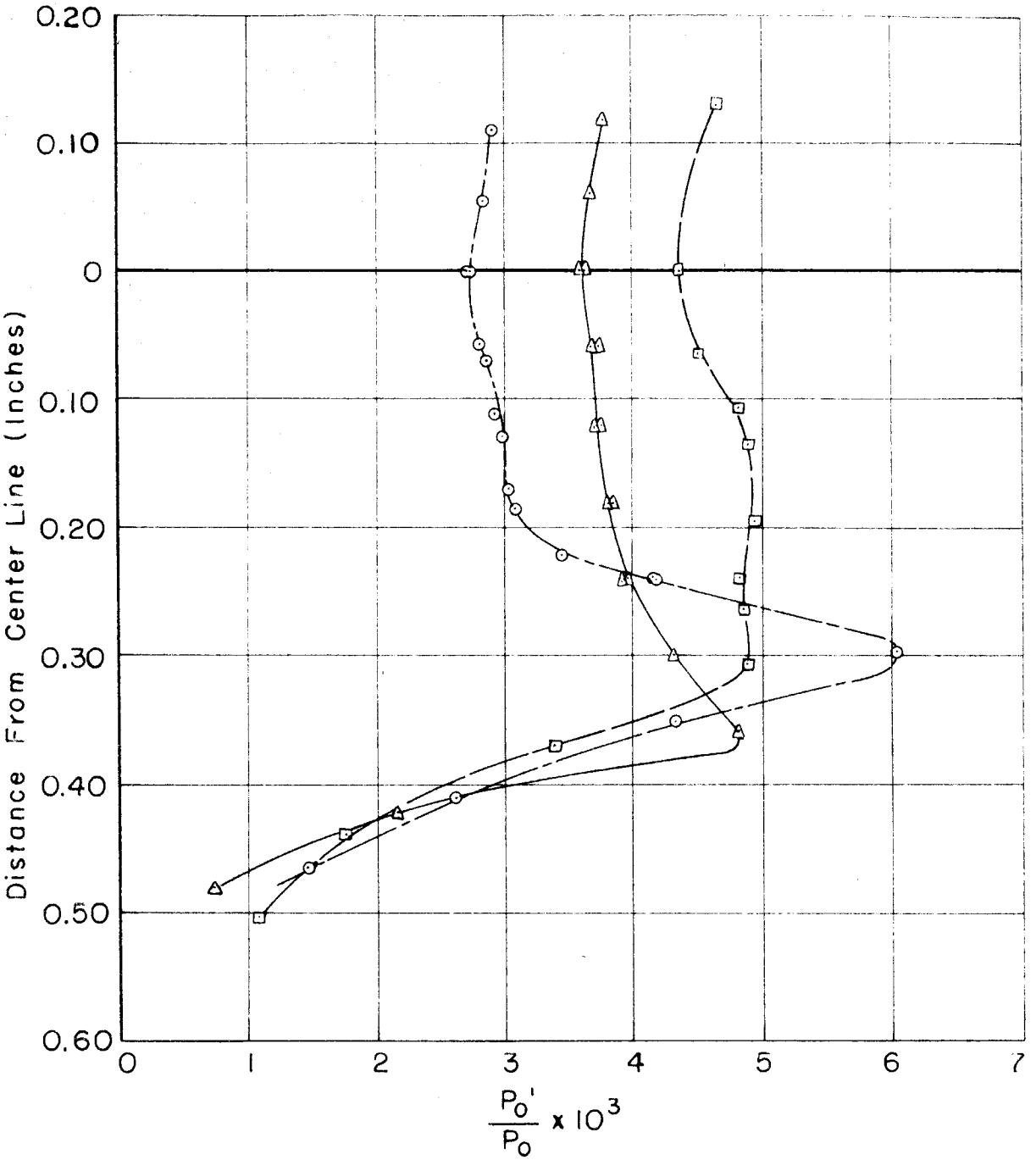

FIG. 4 TOTAL HEAD SURVEYS IN THE TRANSVERSE PLANE FOR VARIOUS AXIAL POSITIONS

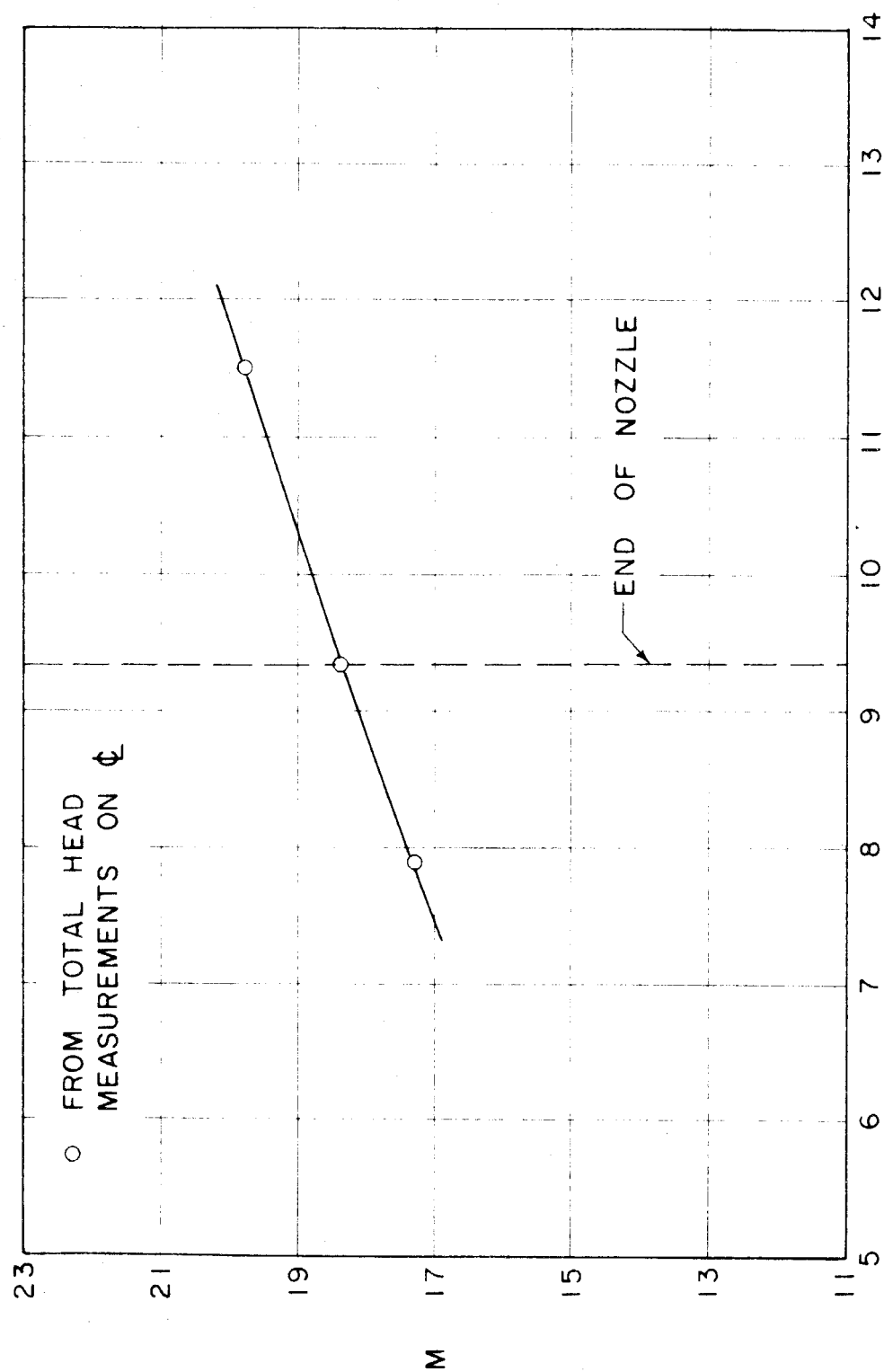

FIG. 5 MACH NUMBER DISTRIBUTION ALONG CENTERLINE OF WIND TUNNEL

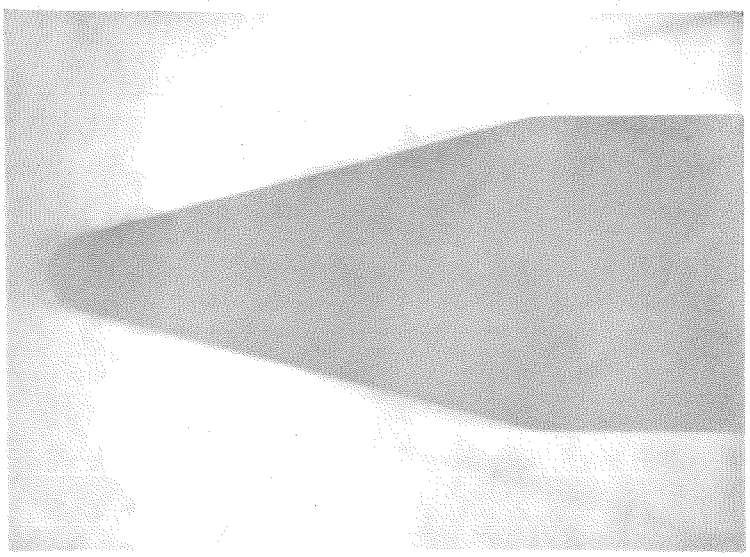

FIGURE 6

SCHLIEREN PHOTOGRAPH OF 15° SPHERICALLY-BLUNT CONE

WITH KNIFE EDGE VERTICAL

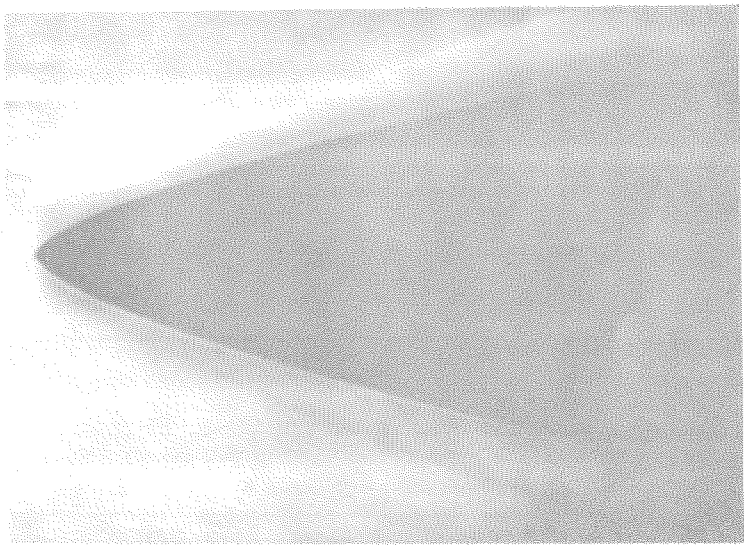

FIGURE 7

SCHLIEREN PHOTOGRAPH OF 2/3 POWER BODY

WITH KNIFE EDGE HORIZONTAL

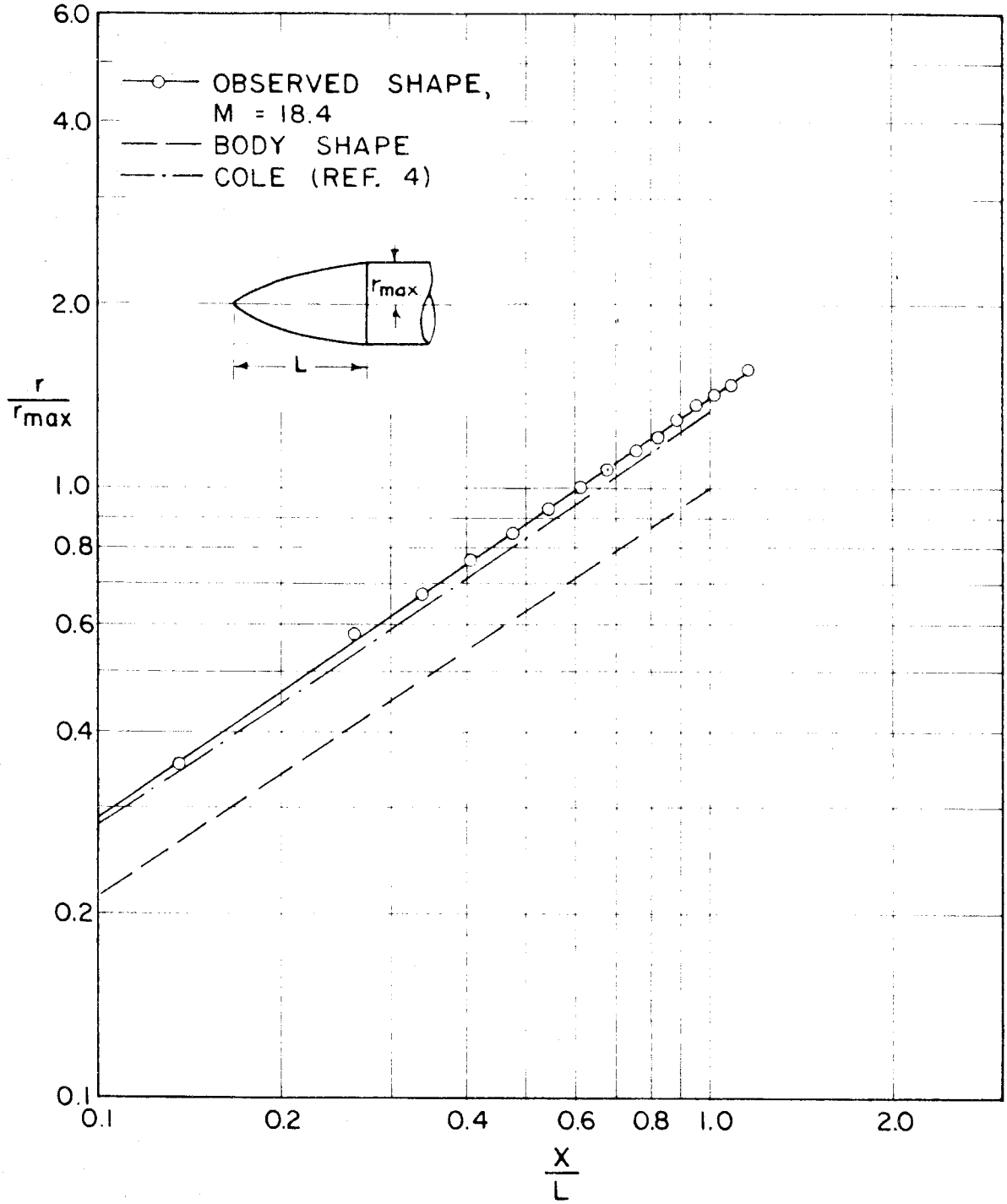

FIG. 8 SHOCK WAVE SHAPE FOR $^2/_3$ POWER BODY

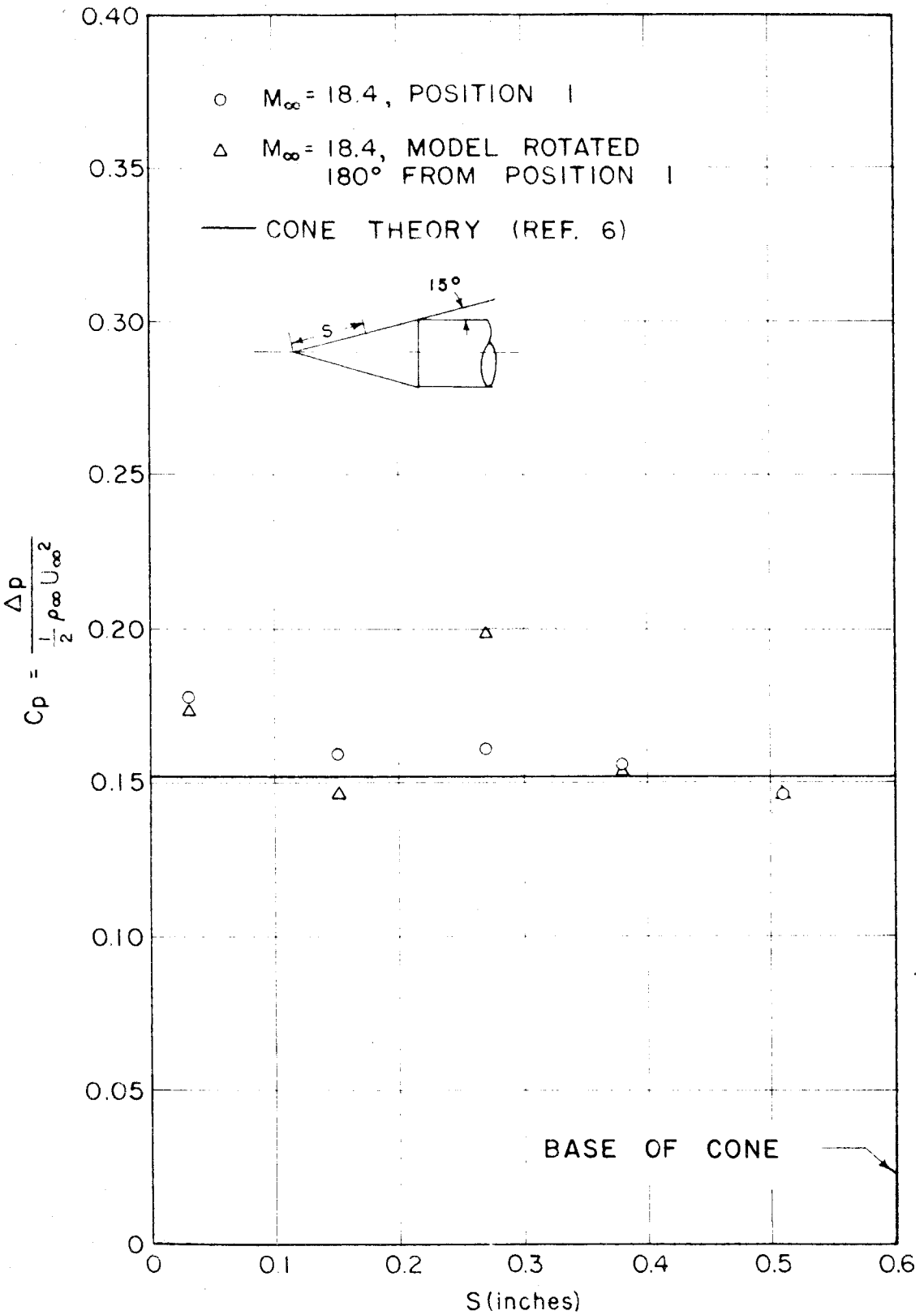

FIG. 9 PRESSURE DISTRIBUTION ON 15° HALF-ANGLE "SHARP" CONE

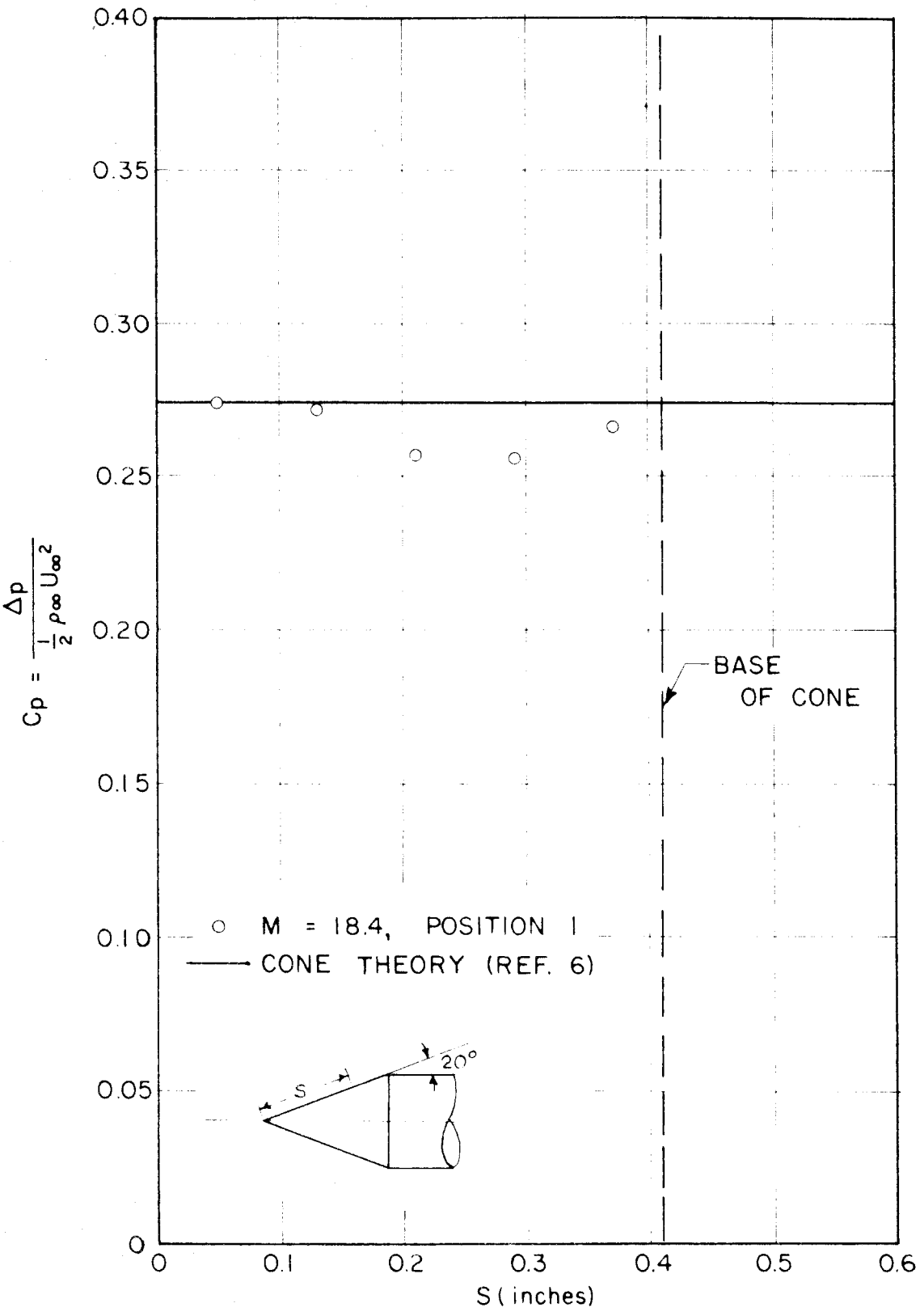

FIG. 10 PRESSURE DISTRIBUTION ON 20° HALF-ANGLE "SHARP" CONE

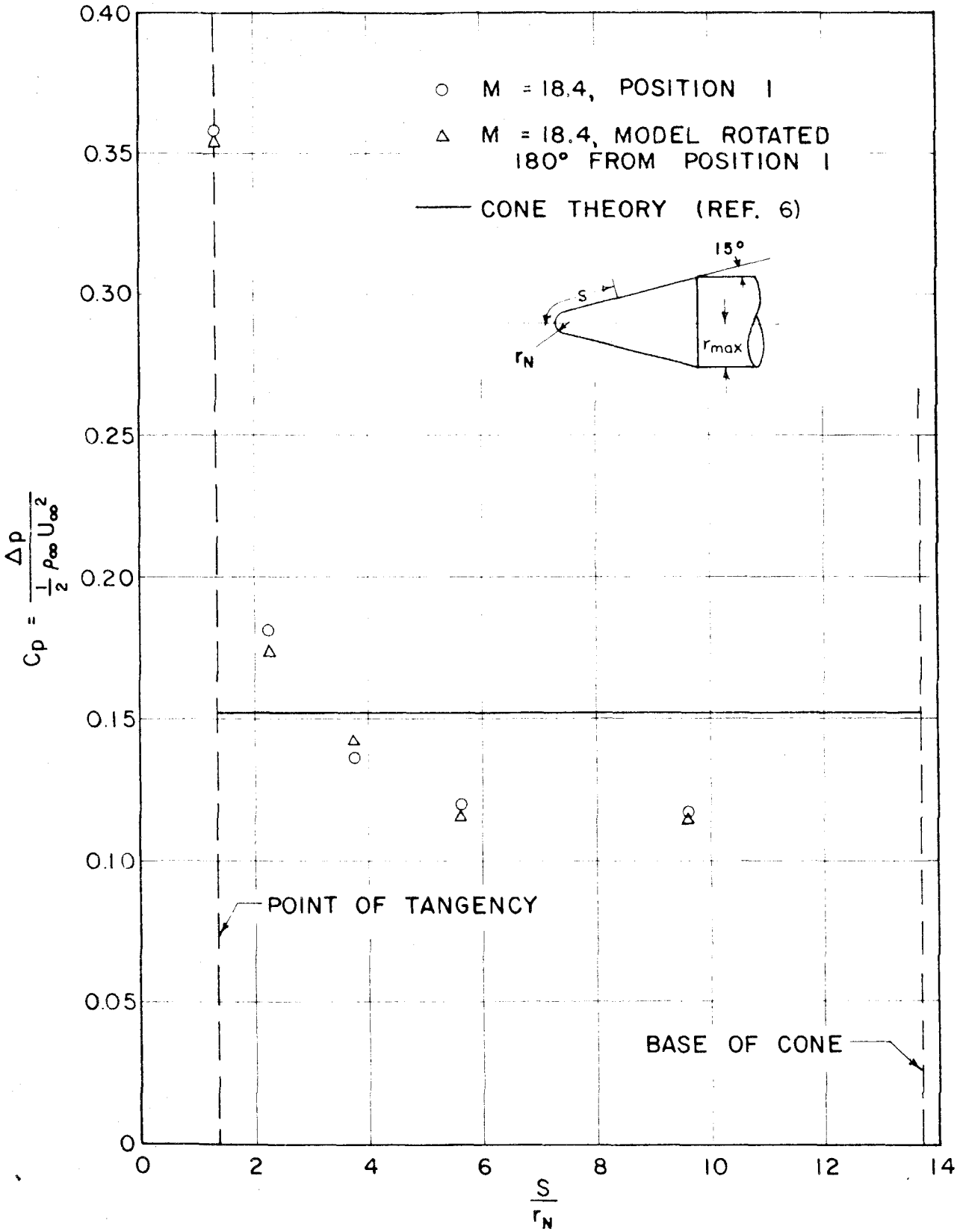

FIG. 11 PRESSURE DISTRIBUTION ON 15° HALF-ANGLE SPHERICALLY-BLUNT CONE, $\frac{r_{max.}}{r_N} = 0.24$